Lin, C., White, R. R., Sparkes, I., & Ashwin, P. (2017). Modeling Endoplasmic Reticulum Network Maintenance in a Plant Cell. *Biophysical Journal*, *113*(1), 214-222. https://doi.org/10.1016/j.bpj.2017.05.046

Biophysical Journal, Volume *113*

Supplemental Information

Modeling Endoplasmic Reticulum Network Maintenance in a Plant Cell

Congping Lin, Rhiannon R. White, Imogen Sparkes, and Peter Ashwin

Supporting Material: Modelling endoplasmic reticulum network maintenance in a plant cell

Congping Lin[1,2,3], Rhiannon R. White[4], Imogen Sparkes[4,5], and Peter Ashwin[3]

[1]Center for Mathematical Sciences, Huazhong University of Science and Technology, Wuhan, China
[2]Hubei Key Lab of Engineering Modelling and Scientific Computing, Huazhong University of Science and Technology, Wuhan, China
[3]Mathematics, University of Exeter, Exeter, UK
[4]Biosciences, University of Exeter, Exeter, UK
[5]School of Biological Sciences, University of Bristol, Bristol, UK

S1 Diffusion rate estimation

The Brownian fluctuations of junction points allow estimation of the diffusion rate of the junction point (and thus an estimation of the viscosity) by evaluating the mean square displacement $MSD(t)$ curve from oscillating junction points in native cells. Linearizing Eq. 2 in the main text near a Steiner point $\bar{x}$ gives $\frac{d}{dt}x = M(x-\bar{x})+\sqrt{2\sigma}\xi(t)$ where $M = b(\nabla_x f)(\bar{x})$ is evaluated at the Steiner point. Assuming persistent points forms equilateral triangle, we have $M = mI$ where I is the identity matrix. Then the $MSD(t)$ for a 2D junction point x under the process $\frac{d}{dt}x = m(x-\bar{x}) + \sqrt{2\sigma}\xi(t)$ near equilibrium follows as below [1]

$$MSD(t) := \lim_{s\to\infty} \langle |x(t+s) - x(s)|^2\rangle = \frac{4\sigma}{m}(1 - e^{-mt})$$

From this, the diffusion rate can be estimated using $4\sigma = \lim_{t\to 0} \frac{d}{dt} MSD(t)$. For the diffusion of ER junction point near equilibrium, we approximate the $MSD(t)$ by considering averages of $|x_i(t + s_k) - x_i(s_k)|^2$ over samples i and over time points s_k and show in Fig. S1 which suggests a diffusion rate of $\sigma \approx 0.002\mu m^2\, s^{-1}$, in a similar order to that estimated in [2] for LatB treated cells (where $\sigma \approx 0.008\mu m^2\, s^{-1}$).

S2 Simulation of network dynamics

The ER network is composed of persistent points (which are immobile), junction points (which are mobile) and tubules between these points that we assume to be straight edges. The model simulates the motion of points and edges as well as any changes through merging and splitting. The model assumes that points will merge if they become too close and then split if this leads to reduction in length: examples of merging and splitting are illustrated in Fig. S2.

For a given set of persistent points, we consider an initial network that connects these points. We use the minimal spanning tree or Delauney triangulation as an initial network state (see Fig. S4 and Movie S2). We then simulate the network dynamics for each time step $h > 0$ as follows.

For the relaxation process P1, we first (P1a) propagate each junction point using an Euler step of duration for a constant time step h according to the resultant tension force (Brownian fluctuations may be included at this point). (P1b) We merge points: if any pair of points is within distance δ, we merge them (merging all to a persistent point if there is one); similarly, if an edge hits a point, then it becomes bound to that point. This involves checking possible intersections between each pair of two edges and the nearest point to the intersection of these edges. (P1c) We delete junction points of degree two (connecting neighboring points) so that all junction points have degree three or more. (P1d) We split persistent or junction points. Any persistent points of degree two or more with an edge angle less than 120^o, or any junction points of degree four or more are split at the smallest edge angle. The splitting is iteratively performed by creating a new junction point at a distance $\epsilon > 0$ from the original point, until all angles at persistent points are at least 120^o (and hence maximum order three) and all junction points are of order three.

For the cross-connection process P2, we randomly add one link with the given cross-connection rate as follows: (P2a) Pick a point on the graph according to a uniform distribution by edge length. (P2b) We pick a random orientation for growth out of the picked point with uniform distribution by angle. (P2s) Finally, we extrapolate a new edge from the chosen point to the first intersection point with another edge: a new edge is created if such intersection exists.

To avoid endless loops of merging and splitting during a single time step, the time step h, distance for merging δ and distance for splitting ϵ must be chosen appropriately. We choose $bh/2 < \delta < \epsilon$ where b is the effective drift velocity of junction points (see main text). For the simulations in this paper we use $b = 1\mu m\, s^{-1}$, $h = 0.02\ s$, $\delta = 0.012\mu m$ (that is about 0.1 multiplication of pixel size in the experimental image) and $\epsilon = 0.024\mu m$ for simulations unless otherwise stated.

S3 Supplementary figures

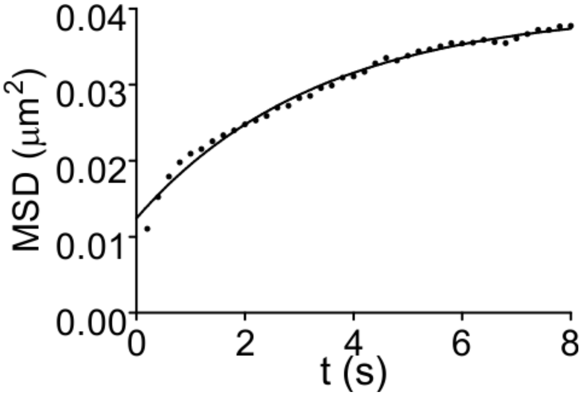

Figure S1: Mean square displacement MSD of ER junction points oscillation around steady state. The $MSD(t)$ is calculated as an average over all possible pair of positions with time lag t among $n = 21$ ER junction point trajectories. Line indicates a fitting to $MSD(t) = \frac{4\sigma}{m}(1 - e^{-mt}) + c$, according to Eq.4 in the main text where c is constant, considering finite spatial resolution and measurement errors of ER junction points.

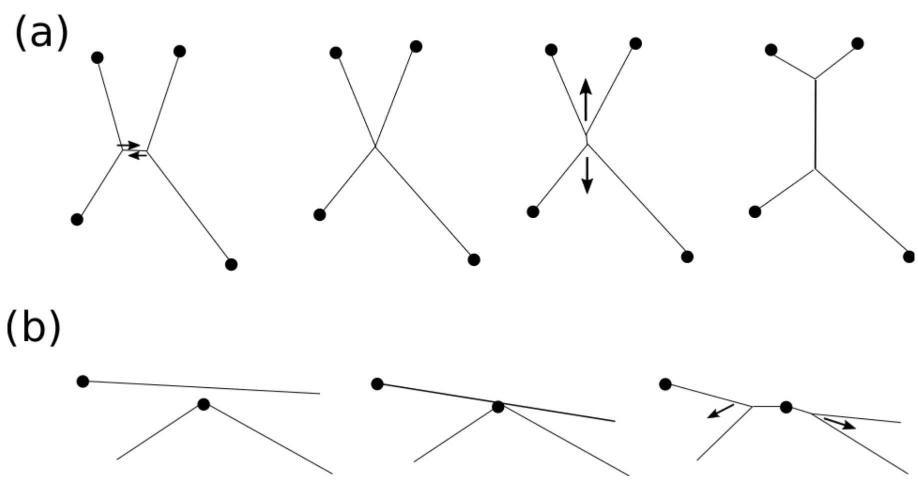

Figure S2: Diagrams showing examples of point splitting and merging that are included as part of P1 in the integrative model. (a) shows an example of the merging of two points that split according to a perturbation that reduces total length. (b) shows a merging between point and an edge that hits the point. This results in a degree four persistent point that splits immediately into two new junction points and a degree two persistent point.

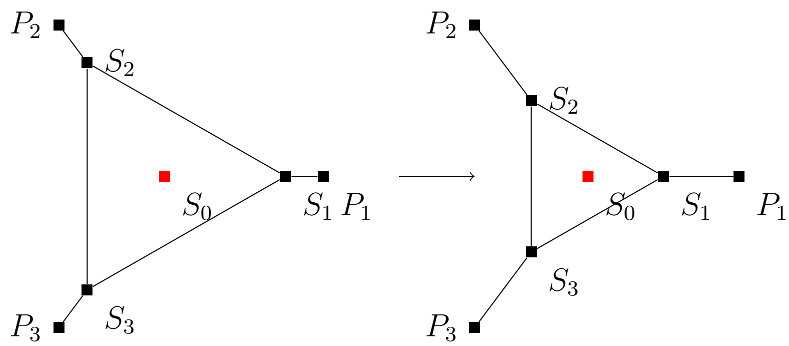

Figure S3: An computable example of a collapsing polygon area in a network between three persistent points P_i , $i = 1, 2, 3$ (forming an equilateral triangle with a center at S_0) and three junction points S_i, $i = 1, 2, 3$ (forming an equilateral triangle with the same center at S_0). S_0 is the Steiner point for persistent points P_1, P_2 and P_3. Using the symmetry and the velocity given by Eq.3 in the main text, the triangle area can be computed as $A(t) = (\sqrt{A_0} - \theta bt)^2$ where $\theta = 3^{3/4}(\sqrt{3} - 1)/2$. This results in collapse of of S_i ($i = 1, 2, 3$) to S_0 (and hence collapse of the triangle) after time $\sqrt{A_0}/(\theta b)$.

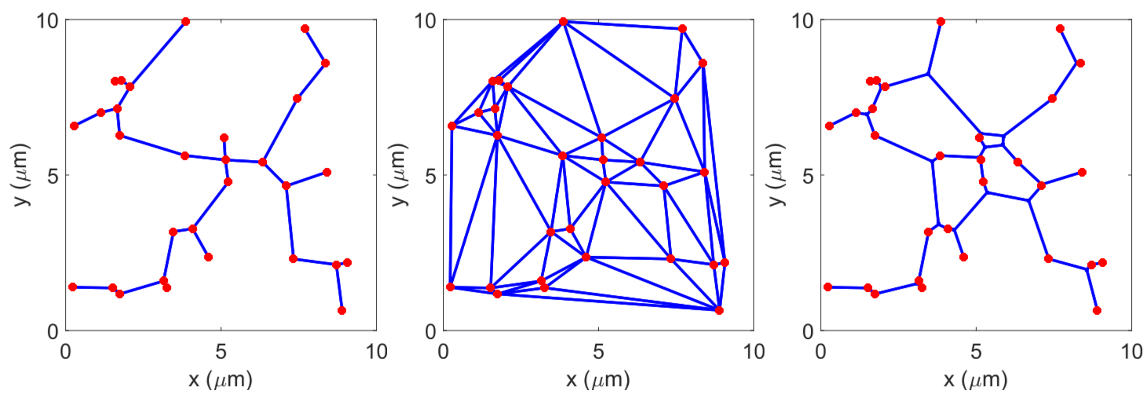

Figure S4: Illustration of two possible initial states of the network, neither of which have any junctions. The minimal spanning tree (left) and Delaunay triangulation (middle) for the same set of 30 persistent points in a $10\mu m \times 10\mu m$ region quickly evolve according to the integrative model towards states that typically have some cycles (right).

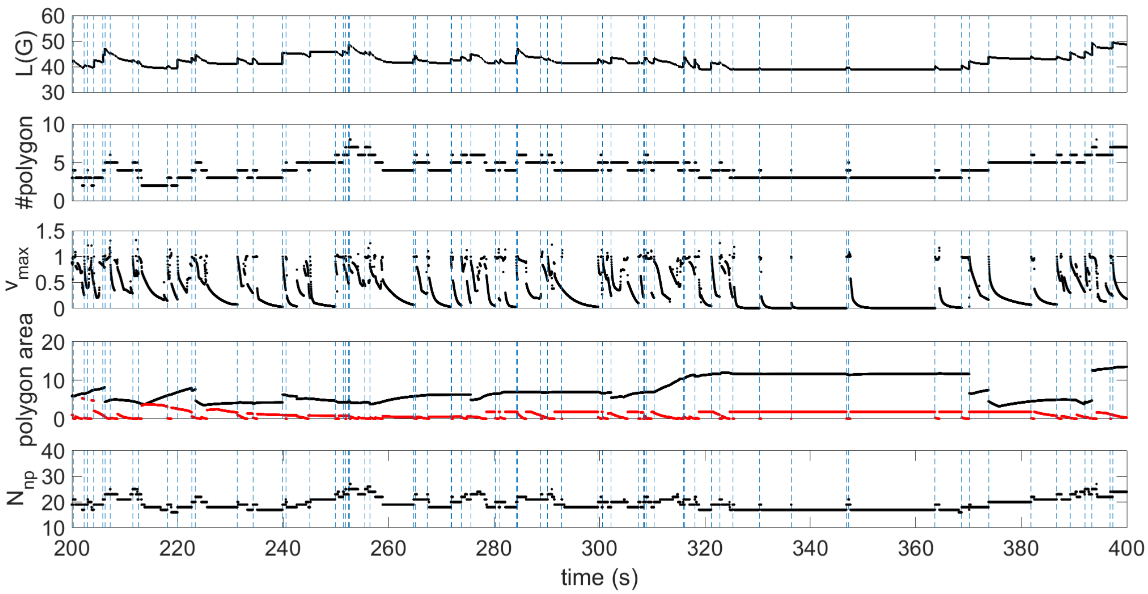

Figure S5: Time series showing the detailed dynamics of various network quantities for a particular realization of the integrative model. From top to bottom the figure shows total network length $L(G) := l(G) \times R$ (where $l(G)$ is the graph length per unit area while R is the area of region), number of polygons, maximal speed of junction points $V_{\max}$, maximal (black curve) and minimal (red) polygon area, and number of junction points N_{np}. We use $\alpha = 0.0048\, s^{-1}$ and $b = 1\mu m\, s^{-1}$ and 30 persistent points distributed randomly across a 10μm×10μm region meaning that area $R = 100\mu m^2$. The fluctuations are induced by the cross connection events (P2) which are at times marked by vertical dashed lines. The relaxation process (P1) results in the decay of $L(G)$ and the $V_{\max}$ after each cross-connection, though the decay of the latter may be non-monotonic due to changes in topology as junction points merge and split.

S4 Movie captions

Movie S1: ER Network Dynamics in Live Tobacco Epidermal Pavement Cells. Shown here is a typical example of ER network dynamics in live tobacco epidermal pavement cells using spinning-disk microscopy.
Movie S2: Network Dynamics Simulated from the Integrative Model. Shown here is an example of network dynamics simulated from the integrative model, starting with minimal spanning tree (left panel) and Delaunay triangulation (right panel) between a set of persistent points in the $10\mu m \times 10\mu m$ region, with parameters $b = 1\mu m\, s^{-1}$ and $\alpha = 0.0048s^{-1}\mu m^{-2}$.
Movie S3: Persistent points of an ER network. Shown here an example of persistent points (red) extracted using the image process method detailed in Materials and Methods on an experimental ER movie in a region of size $13\mu m \times 13\mu m$.
Movie S4: ER Tubular Network Remodeling. An example of ER tubular network remodeling, of $5.54\mu m \times 4.13\mu m$, in a native cell.
Movie S5: Comparison of the Experimental ER Network Dynamics and Network Remodeling from the Model. The network remodeling is simulated from the integrative model, with a drift coeffcient $b = 1\mu m\, s^{-1}$, and new links are added as in the experimental data. The persistent points (red dots) were extracted from the experimental ER movie; the junction points (blue dots) were from the model.
Movie S6: Comparison of the Experimental ER Network Dynamics and Network Remodeling from the Model with Brownian Fluctuations. The network remodeling is simulated from the integrative model with a drift coeffcient $b = 1\mu m\, s^{-1}$, and new link creation as observed from experimental data, together with Brownian uctuations at the estimated diffusion rate $\sigma = 0.002\mu m^2\, s^{-1}$. The persistent points (red dots) were extracted from the experimental ER movie; the junction points (blue dots) were from the model.

Supporting References

[1] Coffey, W. T., and Y. P. Kalmykov. 2012. The Langevin Equation: With Applications to Stochastic Problems in Physics, Chemistry and Electrical Engineering, World Scientific Publishing Company, Singapore.

[2] Lin, C., Y. Zhang, I. Sparkes, P. Ashwin. 2014. Structure and dynamics of ER: minimal networks and biophysical constraints. *Biophys J* 107:763-772.